Time-resolved nondegenerate four-wave mixing in a semiconductor amplifier

W. W. Chow,[1] R. Indik,[2] A. Knorr,[3] S. W. Koch,[2,3,4] and J. V. Moloney[2]
[1]*Sandia National Laboratories, Albuquerque, New Mexico 87185-0601*
[2]*Arizona Center for Mathematical Sciences, University of Arizona, Tucson, Arizona 85721*
[3]*Fachbereich Physik und Zentrum für Materialwissenschaften, Philipps-Universität, Renthof 5, D-35032 Marburg, Germany*
[4]*Optical Sciences Center, University of Arizona, Tucson, Arizona 85721*
(Received 20 December 1994)

The dynamics of copropagating femtosecond pulses with different carrier frequencies is modeled for a semiconductor amplifier. The propagation induced four-wave-mixing signal is studied as a function of the pulse intensity and the spectral detuning between the pulses.

PACS number(s): 42.65.−k, 42.50.Rh

The role of femtosecond pulse propagation dynamics in semicondcutors is a problem of great current interest, both for absorbing and amplifying, i.e., partially inverted systems [1–7]. In this framework, single pulse propagation in semiconductor absorbers and amplifiers has been studied. In semiconductor absorbers temporal polariton formation [4] as well as high-intensity pulse breakup [5] has been observed and confirmed by theoretical calculations. For saturated amplifiers the nonresonantly excited states have been shown to yield important contributions to the pulse shape due to the finite spectral overlap between the pulse spectrum and the dispersive line shape [6]. Propagation effects have been shown to be important not only for single pulse propagation but also in degenerate four-wave-mixing geometries with two input pulses. Here polariton effects in the four-wave-mixing signal in absorbers have been observed and theoretically explained [7].

In this contribution, we study collinear pulse propagation effects using two pulses with different carrier frequencies in nondegenerate four-wave-mixing in semiconductor amplifiers. We use a microscopic theory based on the full Maxwell-semiconductor-Bloch equations (MSBEs) that allows a systematic study of pulse propagation effects, including many-body Coulomb interactions and nonequilibrium carrier population dynamics. The MSBEs consist of two coupled sets of equations: the semiconductor-Bloch equations (SBEs) and the reduced wave equation (RWE). The SBEs are the optical Bloch equations for the interaction of light with a semiconductor medium [8]. They describe the generation of polarization by a light field under the influence of many-body carrier-carrier interactions, while the RWE describes the change of the light field caused by this polarization. Because of its consistent formulation, the MSBE approach provides significant improvement in predictive capability over earlier calculations based on rate equations and phenomenological gain formulas [9–11].

This paper applies the MSBE approach to treat the case of two copropagating pulses. Previous multimode microscopic treatments of the semiconductor gain medium, while accounting for Coulomb interactions, have neglected the effects of propagation, temporal laser field variations and the nonequilibrium population dynamics of the individual electron and hole states [12,13].

The RWE for the propagation of the light field envelope E is given by

$$\frac{\partial E(\eta,\xi)}{\partial \xi} = \frac{i\mu_0\omega_0^2}{k_0 V}\sum_{\vec{q}} P_{\vec{q}}(\eta,\xi), \tag{1}$$

where μ_0 is the permeability, ω_0 is the optical carrier frequency, V is the volume of the gain region, ($\eta = t - z/c$, $\xi = z$) are the retarded time and space coordinates obtained by using a traveling frame at the group velocity c of the pulse, and the summation is over all electron-hole momenta. We use the approximation of slowly varying amplitudes, which is justified because our investigation involves 150-fs pulses, whose pulse envelope E varies slowly in comparison to an optical period. Also, the transverse and lateral dependences of the field are assumed to be given by the guided modes of the amplifier. The source term on the right-hand side is determined by the total polarization $\sum_q P_q$, where each polarization function P_q with electron wave number q obeys the SBEs [8]

$$\frac{\partial P_{\vec{q}}}{\partial \eta} = -i\left(\Delta_{\vec{q}} - \omega_p\right) P_{\vec{q}} - i\Omega_{\vec{q}}\left(f_{\vec{q}}^{e} + f_{\vec{q}}^{h} - 1\right) + \left.\frac{\partial P_{\vec{q}}}{\partial \eta}\right|_{\text{coll}}, \tag{2}$$

$$\frac{\partial f_{\vec{q}}^{e/h}}{\partial \eta} = \left(iP_{\vec{q}}^{*}\Omega_{\vec{q}} + \text{c.c.}\right) + \left.\frac{\partial f_{\vec{q}}^{e/h}}{\partial \eta}\right|_{\text{coll}}. \tag{3}$$

By working in terms of the gain medium polarization instead of invoking the rate equation approximation, the coherent light-semiconductor interactions are treated at a level for superior to the rate equation approach. In the SBE the Rabi frequency of the light is renormalized by Coulomb many-body terms with $\Omega_{\vec{q}} = \frac{d_{cv}E}{2} + \frac{1}{\hbar}\sum_{\vec{q}'} V_{\vec{q}-\vec{q}'}^{S} P_{\vec{q}'}$ where V_q^S is the screened Coulomb potential in Fourier space, which we treat with a quasistatical screening model. Also, the energy dispersion is renormalized by terms proportional to the electron and hole distributions, i.e., $\Delta_{\vec{q}} = \varepsilon_{\vec{q}} - \frac{1}{\hbar}\sum_{\vec{q}'} V_{\vec{q}-\vec{q}'}^{S}\left(f_{\vec{q}'}^{e} + f_{\vec{q}'}^{h}\right) - \frac{1}{\hbar}\sum_{\vec{q}}\left(V_{\vec{q}} - V_{\vec{q}}^{S}\right)$. This renormalization of the single-particle energies is often called band-gap renormalization and, e.g., explains the occurrence of gain below the unexcited semiconductor band gap in an inverted semiconductor.

Besides the terms that result from a time-dependent statically screened Hartree-Fock approximation in the equations of motion, carrier-carrier and carrier-phonon collisions tend to drive the nonequilibrium distribution functions into quasiequilibrium Fermi functions and yield optical dephasing [8]. Within a microscopic description it was shown that the scattering contributions for a certain distribution function depend in general on the distribution and polarization functions of all other single-particle states (non-Markovian behavior) and may show memory effects for very short pulses (less than 100 fs) with respect to the temporal development of the polarization [8,14]. To describe this complicated response behavior, various levels of sophistication have been developed. In this paper, we focus on the propagation of short pulses with relatively small peak power inside the gain region of the amplifier, so that only small deviations of the Fermi functions are caused. It was shown that in this limit, where a reservoir of quasiequilibrium carriers exists, the scattering processes can be approximated within simple relaxation rates [15]. Therefore, the collision terms in our treatment are approximated in the relaxation rate approximation using time constants of 60 fs [15].

To study nondegenerate four-wave-mixing effects we assume two pulses in the sample. We write the initial field as a superposition of two pulses with different center frequencies but with the same temporal shapes and maxima. The temporal envelope of the input pulses is chosen to be sech-like with a peak intensity of 4.5 MW/cm^2 and a full width at half maximum of 150 fs. The spectral width of the pulses is approximately 10 meV. The semiconductor is modeled with the material parameters of GaAs with a total electron-hole density that yields a semiconductor gain width of approximately 100 meV (Fig. 1). To study the influence of propagation effects, the pulses are propagated over ten small signal gain lengths (after one gain length a weak pulse gains e^1 times its initial energy). Solving the above equations numerically, we study the nondegenerate wave-mixing effects as a function of the detuning between the input pulses.

We begin with two input pulses that are strongly detuned with respect to each other. They are centered at ± 20 meV about the unrenormalized band-gap energy. Figures 1(a) and 1(b) show the temporal envelopes and corresponding pulse spectra at different positions in the amplifier. The temporal envelopes show a regular modulation, which is caused by interference effects. In Fig. 1(b), the solid curves show basically equal amplification of both pulses, with negligible change in the spectral shape of each pulse. The small differences in amplification can be attributed to both gain dispersion and differences in the intensities at which the gain is saturated. For comparison, the dashed lines in the figure show single (i.e., noncopropagating) pulse results. The similarity between the solid and dashed curves proves that there is negligible interaction between both pulses under the conditions considered, i.e., detuning of 40 meV. Differences arise because of the increased power density with propagation distance and are not due to cross saturation. There is a redshift in both pulses that increases with propagation distance. This shift, which is small relative to the pulse width, is due to dispersion in the carrier-induced refractive index.

Figure 2 shows the pulse profiles and spectra when the detuning is reduced to 15 meV. The temporal pulse profiles now show strong departures from the regular modulations of the noninteracting case of Fig. 1. Noticeable differences in the amplification of the two pulses appear after a propagation distance of approximately six gain lengths. Distortion of the field spectrum can be noticed after a propagation distance of approximately eight gain lengths. The shoulders on both sides of the two-pulse spectrum are due to the side-mode gain generated by four-wave mixing. They evolve into distinct peaks with further propagation as shown in the spectrum for ten gain lengths. The dominance of the lower-frequency pulse is partially due to gain dispersion, but is also accentuated by mode competition, in the form of spectral hole burning and population pulsation. This conclusion is drawn from comparison with the single pulse propagation studies at detunings of 5 meV and 20 meV from the unexcited

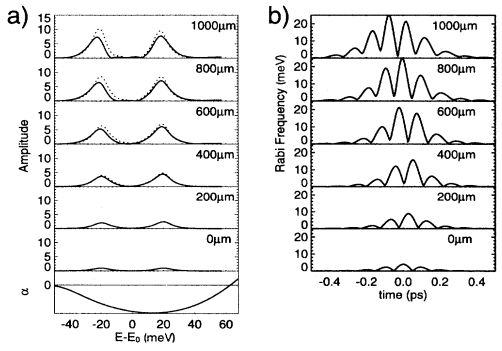

FIG. 1. (a) Pulse temporal profiles and (b) corresponding spectral intensities of two copropagating femtosecond pulses with a total detuning of 40 meV. Dashed lines show results of propagating individual pulses for comparison.

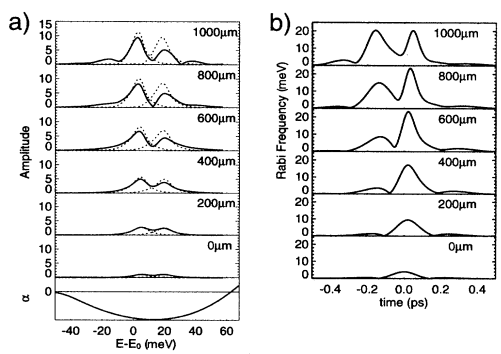

FIG. 2. (a) Pulse temporal profiles and (b) spectral intensities of two copropagating femtosecond pulses with a total detuning of 15 meV. Dashed lines show results of propagating individual pulses for comparison.

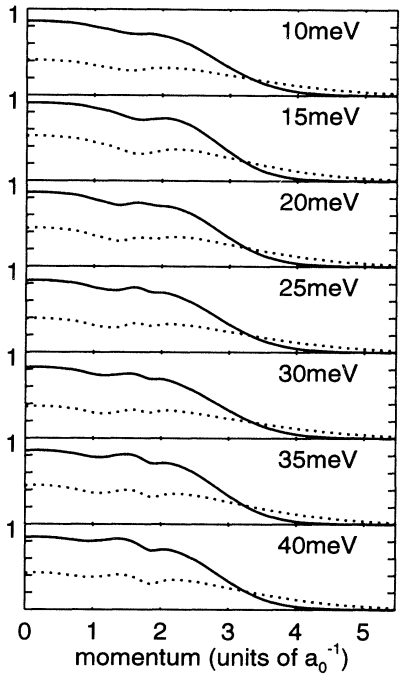

FIG. 3. Distribution of electrons (solid) and holes (dashed) at the pulse peak measured after propagating ten gain lengths.

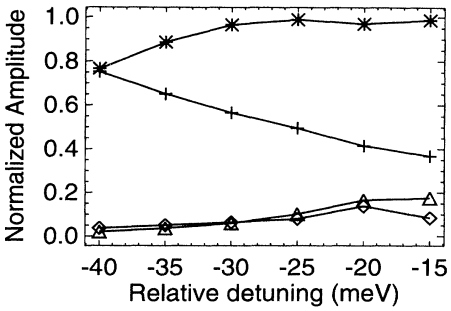

FIG. 4. Normalized signal and sideband intensities (*, at ν_1; +, at ν_2; △, at the lower sideband; ◇, at the upper sideband) as a function of pulse detuning after propagating ten gain lengths. The signal intensities are normalized with respect to the single pulse intensities at ν_2.

bulk GaAs band gap and from plots of the carrier distributions. Figure 3 shows the spectral holes in the carrier distributions at the end of the amplifier. The spectral holes in each distribution (electrons and holes) associated with the strongly detuned individual pulses merge together around a detuning of 15 meV, signifying direct competition for gain with subsequent degradation of each pulse identity.

To understand the coherent saturation effects (i.e., those not due to spectral hole burning), we consider the interaction of the two pulses as mediated by the nonlinear amplifier medium. For optical pulses that are sufficiently intense to saturate the gain medium, the nonlinear interaction of light and semiconductor generates density pulsations that are driven by the product of the fields: $E_1 E_2 \cos(\Delta t)$, where Δ is the detuning between the two pulses. These density oscillations generate polarizations oscillating at $\nu_1 \pm \Delta$ and $\nu_2 \pm \Delta$, where ν_1 (ν_2) is the frequency of the lower- (higher-) frequency pulse. The $\nu_1 + \Delta$ and $\nu_2 - \Delta$ polarizations enhance or deplete the gain at ν_2 and ν_1, respectively, depending on their phases relative to those of the pulses. Together with spectral hole burning, these polarizations due to population pulsations contribute to cross-mode saturation. The four-wave-mixing contributions come from the polarizations at the new frequencies $\nu_1 - \Delta$ and $\nu_2 + \Delta$ [16].

Finally, Fig. 4 plots the normalized output intensities at ν_1, ν_2, $\nu_1 - \Delta$, and $\nu_2 + \Delta$ as a function of detuning, $\hbar\Delta$. The figure shows a significant decrease in the output intensity for $\nu = \nu_2$ and an increase in side-mode outputs for detuning less than half the gain bandwidth. For higher detuning, the spectral holes of the pulses do not overlap and the gain bandwidth is not sufficiently broad to provide gain to the side modes. Consequently, there is negligible distortion of the input pulse spectrum. The situation drastically changes when the detuning between the pulses is decreased so that the side-mode frequencies fall inside the gain region.

In summary, our analysis shows multimode gain nonlinearities in an amplifying semiconductor medium in the transient regime. The nonlinearities appear in the form of cross-mode saturation via spectra hole burning and population pulsations, and frequency conversion via nondegenerate four-wave mixing. The microscopic treatment of the gain medium allows the self-consistent description of the effects of the band structure, many-body Coulomb interactions, and the nonequilibrium carrier dynamics. We show that by changing the frequency difference between two copropagating laser pulses, the strength of the optical nonlinearities may be varied. This allows systematic investigations of their behaviors, which may be helpful in understanding the physical limitations of semiconductor lasers and amplifiers in applications such as multichannel optical communications.

Support for this work is acknowledged from the U.S. Department of Energy through Contract No. DE-AC04-94AL85000, the Arizona Center for Mathematical Sciences under Grant No. AFOSR F49620-94-1-0014DEF, with partial support from the Optical Circuitry Cooperative, University of Arizona, and the Deutsche Forschungsgemeinschaft partially through the Sonderforschungsbereich 383. Computing support was provided by the AHPCRC at the Minnesota Supercomputer Center and by HLRZ, Jülich. We acknowledge support under the NATO international scientific exchange program.

[1] G. Grosskopf, R. Ludwig, R. G. Waarts, and H. G. Weber, Electron. Lett. **24**, 31 (1988).
[2] W. Schäfer and K. Henneberger, Phys. Status Solidi B **159**, 59 (1990).
[3] A. Knorr, R. Binder, M. Lindberg, and S. W. Koch, Phys. Rev. A **46**, 7179 (1992).
[4] D. Fröhlich, A. Kulik, B. Uebbing, A. Mysyrowicz, V. Langer, H. Stolz, and W. von der Osten, Phys. Rev. Lett. **67**, 2343 (1991).
[5] P. A. Harten, A. Knorr, J. P. Sokoloff, F. Brown de Coulston, S. G. Lee, R. Jin, E. M. Wright, G. Khitorova, H. M. Gibbs, S. W. Koch, and N. Peyghambarian, Phys. Rev. Lett. **69**, 852 (1992).
[6] A. Knorr, R. Binder, E. M. Wright, and S. W. Koch, Opt. Lett. **18**, 1538 (1993); R. Indik, A. Knorr, R. Binder, J. V. Moloney, and S. W. Koch, Opt. Lett. **19**, 966 (1994).
[7] T. Rappen, G. Mohs, and M. Wegener, Phys. Rev. B **47**, 9658 (1993).
[8] M. Lindberg and S. W. Koch, Phys. Rev. B **38**, 3342 (1988); W. Schäfer, *Festkörperprobleme,* edited by U. Rössler (Vieweg, Braunschweig, 1988), Vol. 28, p. 63; S. Schmitt-Rink, D. S. Chemla, and H. Haug, Phys. Rev. B **37**, 941 (1988); R. Zimmermann and M. Hartmann, Phys. Status Solidi B **38**, 3342 (1988); I. Balslev, R. Zimmermann, and A. Stahl, Phys. Rev. B **40**, 4095 (1989), for further discussion see H. Haug and S. W. Koch, *Quantum Theory of the Optical and Electronic Properties of Semiconductors*, 2nd ed. (World Scientific, Singapore, 1993).
[9] T. Mukai and T. Saitoh, IEEE J. Quantum Electron. **QE-26**, 865 (1990).
[10] F. Favre and D. LeGuen, IEEE J. Quantum Electron. **QE-26**, 858 (1990).
[11] G. P. Agrawal, J. Opt. Soc. Am. B **5**, 147 (1988).
[12] F. L. Zhou, M. Sargent III, S. W. Koch, and W. W. Chow, Phys. Rev. A **41**, 463 (1990).
[13] M. Sargent, S. W. Koch, and W. W. Chow, J. Opt. Soc. Am. B **9**, 1288 (1992).
[14] W. Schäfer and J. Treusch, Z. Phys. B **63**, 407 (1986); H. Haug, Phys. Status Solidi B **173**, 139 (1992); D. B. Tran Thoai and H. Haug, *ibid.* **173**, 159 (1992); W. Schäfer, *Optics of Semiconductor Nanostructures*, edited by F. Henneberger, S. Schmitt-Rink, and E. O. Göbel (Akademie-Verlag, Berlin, 1993), and references cited therein; K. E. Sayed, S. Schuster, H. Haug, F. Herzel, and K. Henneberger, Phys. Rev. B **49**, 7337 (1994).
[15] R. Binder, D. Scott, A. Paul, M. Lindberg, K. Henneberger, and S. W. Koch, Phys. Rev. B **45**, 1107 (1992).
[16] See, e.g., W. W. Chow, S. W. Koch, and M. Sargent, *Semiconductor Laser Physics* (Springer-Verlag, Berlin, 1994), Chap. 8.